Large Tunneling Magnetoresistance in GaMnAs/AlAs/GaMnAs Ferromagnetic Semiconductor Tunnel Junctions

M. Tanaka and Y. Higo

Department of Electronic Engineering, University of Tokyo, 7-3-1 Hongo, Bunkyo-ku, Tokyo 113-8656, Japan

(Received 5 January 2001; published 22 June 2001)

We have observed very large tunneling magnetoresistance (TMR) in epitaxially grown $Ga_{1-x}Mn_xAs/AlAs/Ga_{1-x}Mn_xAs$ ferromagnetic semiconductor tunnel junctions. Large TMR ratios more than 70% (maximum 75%) were obtained in junctions with a very thin ($\leq$1.6 nm) AlAs tunnel barrier when the magnetic field was applied along the [100] axis in the film plane. The TMR was found to rapidly decrease with increasing barrier thickness, which is explained by calculations assuming that the parallel wave vector of carriers is conserved in tunneling.

DOI: 10.1103/PhysRevLett.87.026602 PACS numbers: 72.25.Dc, 73.40.Gk, 75.50.Pp, 75.70.Pa

In the past few years, tunneling magnetoresistance (TMR) and related phenomena were extensively studied in magnetic tunnel junctions (MTJs) [1,2], leading to important applications such as magnetic field sensors and magnetic random access memory. In most of the experiments on spin-polarized tunneling in ferromagnet/insulator/ferromagnet (FM/I/FM) tunnel junctions, polycrystalline transition metals and amorphous oxides are used as FM and I layers, respectively.

On the other hand, ferromagnetic semiconductor heterostructures based on $Ga_{1-x}Mn_xAs$ can provide a new opportunity to study spin-dependent transport phenomena. Because $Ga_{1-x}Mn_xAs$ is a ferromagnetic p-type semiconductor with the zinc-blende–type crystal structure having almost the same lattice constant as GaAs and AlAs, $Ga_{1-x}Mn_xAs$/III-V heterostructures can be epitaxially grown with abrupt interfaces and with atomically controlled layer thicknesses [3–5]. Although the Curie temperature of $Ga_{1-x}Mn_xAs$ is below room temperature thus far (at most 110 K [4]), using $Ga_{1-x}Mn_xAs$-based III-V heterostructures as tunnel junctions would have several advantages: (i) One can form high-quality single-crystalline MTJs made of all-semiconductor heterostructures, which can be easily integrated with other III-V–based structures and devices. (ii) Many structural and band parameters are controllable. (iii) Introduction of quantum heterostructures is easier than any other material system [6]. However, little is understood of the spin-polarized tunneling in such ferromagnetic semiconductor heterostructure systems. Also, little is experimentally clarified in such all-epitaxial monocrystalline MTJs.

We recently observed TMR in a $Ga_{1-x}Mn_xAs/AlAs/Ga_{1-x}Mn_xAs$ MTJ with a magnetic field applied in plane along the [110] direction [7]. Although the total change in the tunnel resistance at 4.2 K was 44%, including the slowly saturating negative component at higher magnetic field, the TMR ratio purely due to the spin-valve effect was estimated to be only 15%–19% [7]. More recently, Chiba *et al.* [8] also reported a TMR ratio of 5.5% at 20 K in a $Ga_{1-x}Mn_xAs/AlAs/Ga_{1-x}Mn_xAs$ trilayer.

In this Letter, we report on by far larger TMR ratios (>70%) at 8 K in $Ga_{1-x}Mn_xAs/AlAs/Ga_{1-x}Mn_xAs$ tunnel junctions, which are due purely to the change of the magnetization direction of the two electrodes. The TMR ratio was found to rapidly decrease with increasing the barrier thickness d_{AlAs} in junctions with $d_{\mathrm{AlAs}} > 1.5$ nm. This barrier thickness dependence of the TMR can be explained by tight-binding calculations of tunneling assuming that the wave vector of carriers in the direction parallel to the interface is conserved.

Figure 1(a) illustrates the sample structure prepared by low temperature–molecular beam epitaxy (LT-MBE). After a 100-nm-thick Be-doped (2.6×10^{18} cm^{-3}) p^+-GaAs buffer layer was grown at 580 °C on a p^+-GaAs (001) substrate, a $Ga_{1-x}Mn_xAs$ ($x = 4.0\%, 50$ nm)/AlAs (d_{AlAs})/$Ga_{1-x}Mn_xAs$ ($x = 3.3\%, 50$ nm) trilayer was grown at 250 °C. By using a shutter linearly moving in front of the substrate, we prepared a wedge-type sample, in which the barrier thickness d_{AlAs} was changed within a wafer of 20×20 mm^2. Undoped 1-nm-thick GaAs spacers were inserted between $Ga_{1-x}Mn_xAs$ and AlAs to avoid Mn diffusion into the barrier and to make the interfaces smooth. In order to measure tunneling transport, the sample was patterned with photolithography into arrays of round-shaped junctions 200 μm in diameter with various d_{AlAs} ranging from 1.3 to 2.8 nm.

The magnetization of a $Ga_{1-x}Mn_xAs$ ($x = 4.0\%$, 50 nm)/AlAs (3 nm)/$Ga_{1-x}Mn_xAs$ ($x = 3.3\%, 50$ nm) trilayer measured by SQUID at 8 K is shown in Fig. 1(b). The specimen size was 3×3 mm^2, and the magnetic field was applied along the [100] axis in the plane. Because of the different coercivity of the two $Ga_{1-x}Mn_xAs$ layers, we observed a double-step magnetization curve with coercive fields of about 60 and 100 Oe. Pairs of arrows in the figure indicate the configuration of the two magnetizations.

Figure 1(c) shows tunnel resistance vs magnetic field, that is, TMR curves measured at 8 K on a junction with

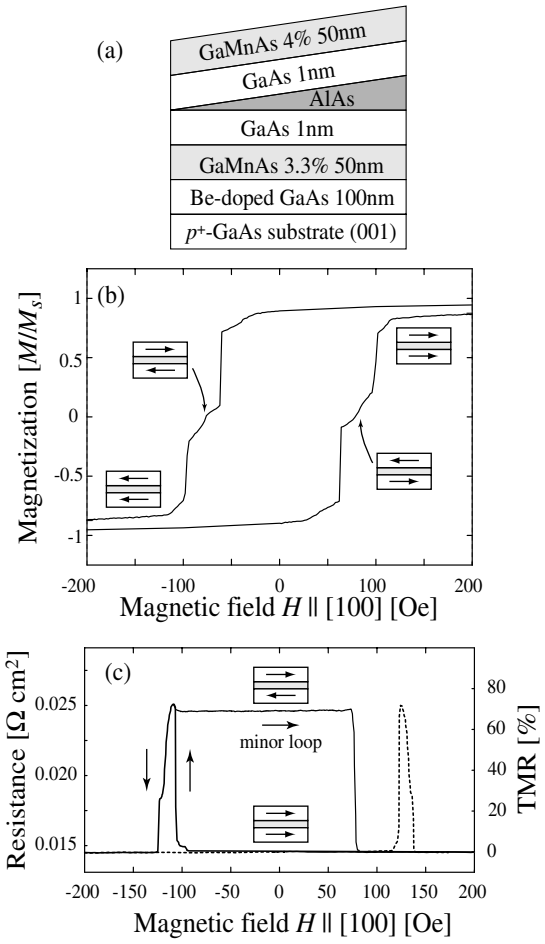

FIG. 1. (a) Schematic illustration of a wedge-type ferromagnetic semiconductor trilayer heterostructure sample grown by LT-MBE. (b) Magnetization of a $Ga_{1-x}Mn_xAs$ ($x = 4.0\%, 50$ nm)/AlAs (3 nm)/$Ga_{1-x}Mn_xAs$ ($x = 3.3\%$, 50 nm) trilayer measured by SQUID at 8 K. The specimen size was 3×3 mm^2. The vertical axis shows the normalized magnetization M/M_s, where M_s is the saturation magnetization. (c) TMR curves at 8 K of a $Ga_{1-x}Mn_xAs$ ($x = 4.0\%, 50$ nm)/AlAs (1.6 nm)/$Ga_{1-x}Mn_xAs$ ($x = 3.3\%, 50$ nm) tunnel junction 200 μm in diameter. Bold solid and dashed curves were obtained by sweeping the magnetic field from positive to negative and negative to positive, respectively. A minor loop is shown by a thin solid curve. In both (b) and (c), the magnetic field was applied along the [100] axis in the plane.

$d_{\mathrm{AlAs}} = 1.6$ nm when the magnetic field was applied along the [100] axis in the plane. The measurements were done at a constant bias of 1 mV, and so there is no hot-carrier effect. The TMR is defined here as $[R(H) - R(0)]/R(0)$, where $R(H)$ is the resistance at the field of H, and $R(0) = 0.015\ \Omega$ cm^2 taken from a major loop. Bold solid and dashed curves (major loop) in Fig. 1(c) were obtained by sweeping the field from positive to negative and negative to positive, respectively. When the magnetization directions of the two $Ga_{1-x}Mn_xAs$ layers are parallel, $R(H)$ is 0.015 Ω cm^2. $R(H)$ increased to 0.025 Ω cm^2 (corresponding TMR was 72%) at $H = -110 \sim -120$ Oe (solid curve) and $H = 120 \sim 130$ Oe (dashed curve), when the magnetizations of the $Ga_{1-x}Mn_xAs$ layers became antiparallel. The difference in the coercive fields between the M-H curve in Fig. 1(b) and the TMR curve in Fig. 1(c) is caused by the difference in the shape and size of the measured specimens. Note that the TMR value is over 70%, much higher than the TMR previously reported [7,8]. A thin solid curve in Fig. 1(c) shows a minor loop, indicating that the antiparallel configuration is stable, as well as the parallel configuration.

Figure 2(a) shows the tunnel resistance R for the junctions measured at 8 K as a function of the barrier thickness

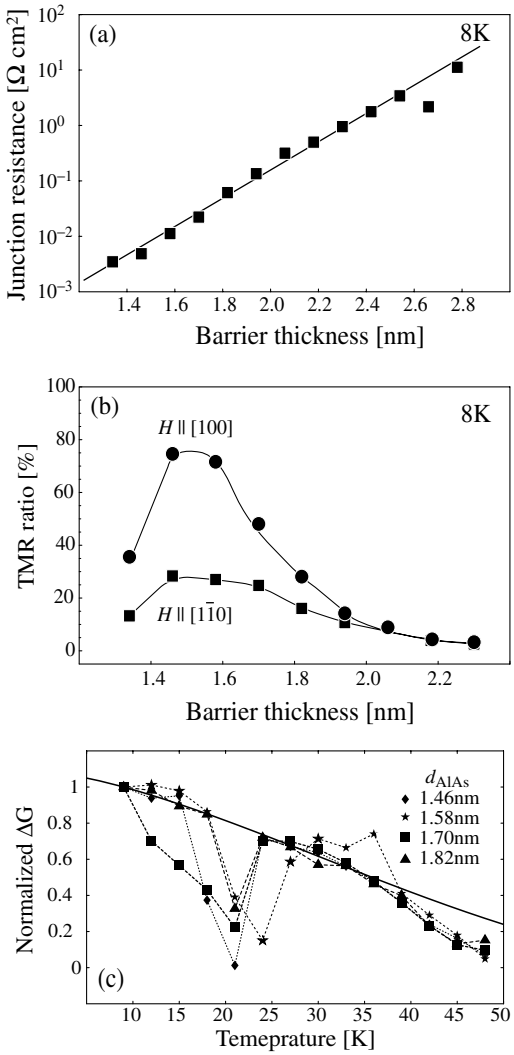

FIG. 2. Barrier thickness dependence of (a) the tunnel resistance and (b) the TMR in $Ga_{1-x}Mn_xAs$ ($x = 4.0\%$, 50 nm)/AlAs (d_{AlAs})/$Ga_{1-x}Mn_xAs$ ($x = 3.3\%, 50$ nm) tunnel junctions measured at 8 K. In (b), the TMR values were measured with the magnetic field applied along the [100] and [1$\bar{1}$0] axes. (c) Temperature dependence of normalized conductance difference ΔG for various junctions with $d_{\mathrm{AlAs}} = 1.46$, 1.58, 1.70, and 1.82 nm. The solid line in (c) is the fit to the theory based on thermal spin-wave excitations.

d_{AlAs}. The resistance exponentially increased from 10^{-3} to 10 $\Omega\,\mathrm{cm}^2$ as d_{AlAs} increased, which means that high-quality tunnel junctions were formed with a constant barrier height. In the WKB approximation, the slope of $\ln R - d_{\mathrm{AlAs}}$ characteristics is given by $2\sqrt{2m^*V_b}/\hbar$, thereby the product m^*V_b is estimated to be $0.32m_0$ [kg eV], where m_0 is the free-electron mass, m^* is the effective mass of holes, and V_b is the barrier height [9].

Figure 2(b) shows barrier thickness dependence of TMR at 8 K when the magnetic field was applied in plane along the [100] and [1$\bar{1}$0] axes. The maximum TMR was 75% at $d_{\mathrm{AlAs}} = 1.46$ nm when the field was applied along the [100] axis. In both field directions, with increasing d_{AlAs} (>1.5 nm), the TMR was found to rapidly decrease from the maximum value at $d_{\mathrm{AlAs}} = 1.46$ nm. At all the values of d_{AlAs}, the TMR was higher when the field was applied along the [100] axis than along the [1$\bar{1}$0] axis. The difference in the TMR between the two field directions is due to the cubic magnetocrystalline anisotropy induced by the zinc-blende–type $Ga_{1-x}Mn_xAs$ crystal structure, where the easy magnetization axis of $Ga_{1-x}Mn_xAs$ is ⟨100⟩, the detail of which is reported elsewhere [10]. Although the reason for the drop in the TMR for the junction with $d_{\mathrm{AlAs}} < 1.4$ nm is not clear at present, this drop could be caused by the ferromagnetic interlayer exchange coupling between $Ga_{1-x}Mn_xAs$ layers separated by a thin AlAs layer [8].

We also measured the temperature dependence of the TMR for various junctions with different d_{AlAs}, and plotted in Fig. 2(c) the normalized conductance difference $\Delta G = \Delta G(T)/\Delta G(8\ \mathrm{K})$, where $\Delta G(T) = G_{\mathrm{P}}(T) - G_{\mathrm{AP}}(T)$, $G_{\mathrm{P}}(T)$ and $G_{\mathrm{AP}}(T)$ are the junction conductances at T [K] for parallel and antiparallel magnetization, respectively. ΔG (equivalently, TMR) basically decreased with increasing temperature and vanished at ~50 K, which is the Curie temperature of one of the $Ga_{1-x}Mn_xAs$ layers. ΔG dropped once, at $T \sim 20$ K, because the coercivity of the top and bottom GaMnAs layers is so close (almost the same) that the window for antiparallel magnetization is too small, which was confirmed by temperature-dependent magnetization measurements, thus G_{AP} was difficult to be observed at around 20 K. The solid line in Fig. 2(c) is the fit to the theory $\Delta G(T) = \Delta G_0(1 - \alpha T^{3/2})^2$, where ΔG_0 is a constant and α is fitted to 1.5×10^{-3} [$\mathrm{K}^{-3/2}$], based on thermal spin-wave excitations [11]. The theory can explain the present data, as it did for conventional $Co/Al_2O_3/Co$(NiFe) MTJs [11]. This means that the dominant contribution to the tunnel conductance is direct elastic tunneling with the tunneling carrier spin-polarization P decreasing as $1 - \alpha T^{3/2}$.

In Jullière's model [12], the TMR depends only on the spin-dependent density of states in the two FM electrodes and does not depend on the barrier thickness d; therefore the Jullière model cannot explain our experimental results. Because the present heterostructures are epitaxially grown single crystals, the wave vector $\mathbf{k}_\parallel$ of carriers parallel to the interface should be conserved in tunneling. Calculations using the tight-binding theory [13], including $\mathbf{k}_\parallel$ conservation, seem consistent with our results.

Our experimental results can be qualitatively explained as follows: Figure 3 shows the Fermi surfaces for up and down spins in two FM electrodes, calculated by the single-orbital tight-binding model, when the two magnetizations are 3(a) parallel and 3(b) antiparallel. Also, the calculated dispersion of the decaying factor κ_z in the barrier is shown in the middle of the figure. The wave vector $k_z(E_F, \mathbf{k}_\parallel)$ normal to the interface in the FM electrodes is determined from $E_F = E_0 + 2t\cos(k_z a) + w(\mathbf{k}_\parallel)$, and the decaying factor $\kappa_z(E_F, \mathbf{k}_\parallel)$ in the barrier layer is determined from $E_F = E_0 + 2t\cosh(\kappa_z a) + w(\mathbf{k}_\parallel)$, where $w(\mathbf{k}_\parallel) = 2t[\cos(k_x a) + \cos(k_y a)]$, $\mathbf{k}_\parallel = (k_x, k_y)$ is the wave vector parallel to the film plane, E_F is the Fermi energy, E_0 is the on-site energy in each layer, t is the nearest-neighbor hopping parameter, and a is the lattice constant [13]. We simply regard spin polarization in the FM electrodes in the difference of E_0 between the majority and minority carriers. In parallel magnetization [Fig. 3(a)], the majority (minority) spin is the up (down) spin in both electrodes, so that the carriers can tunnel through all the channels $(\mathbf{k}_\parallel, \sigma)$. In antiparallel magnetization [Fig. 3(b)], the down spin is the majority spin in the right electrode, thus the carriers with $k_\parallel = |\mathbf{k}_\parallel| > k_{\mathrm{cutoff}}$ cannot tunnel (k_{cutoff} is the largest $k_\parallel$ in the minority spin band). This difference in tunneling between the parallel and antiparallel configurations indicates

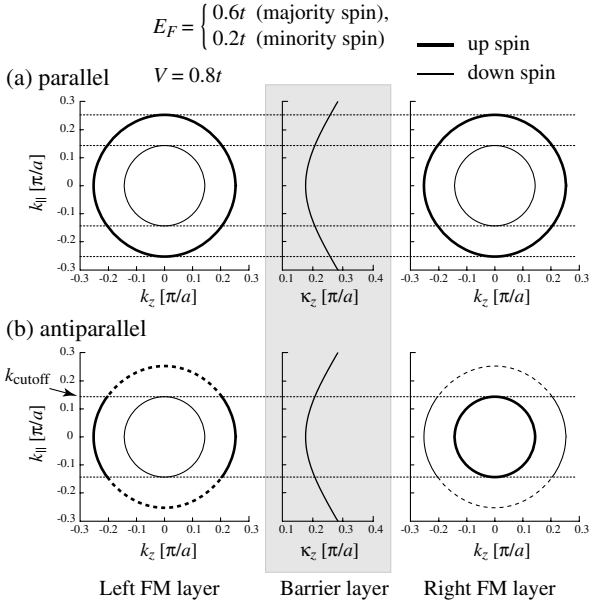

FIG. 3. Fermi surfaces for up and down spins of the left and right FM electrodes in (a) parallel and (b) antiparallel magnetization configurations, calculated by the single-orbital tight-binding model. Dependence of the decaying factor κ_z on $k_\parallel$ is also shown in the middle of the figure.

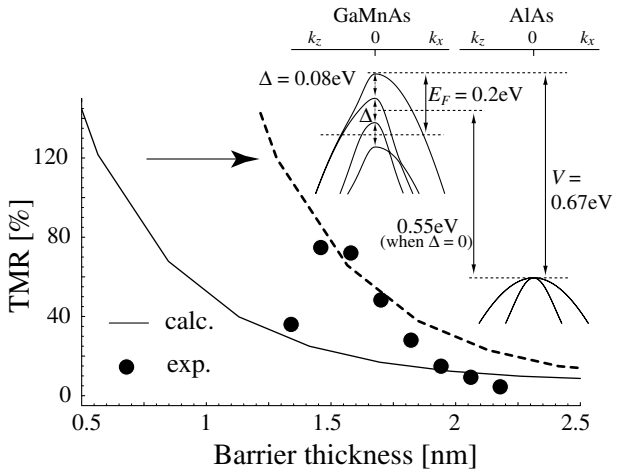

FIG. 4. The solid curve represents the calculated dependence of TMR on the barrier thickness when the Fermi energy $E_F = 0.2$ eV, the barrier height $V = 0.67$ eV (both measured from the top of the valence band of $Ga_{1-x}Mn_xAs$), and the spin splitting $\Delta = 0.08$ eV between the two light holes $|\frac{3}{2}, \frac{1}{2}\rangle$ and $|\frac{3}{2}, -\frac{1}{2}\rangle$ at the Γ point. The inset shows the valence band dispersion and the relationship of these parameters. The solid curve is horizontally shifted by 0.7 nm to the dashed curve to fit the experimental results (solid circles, the magnetic field was along the [100] axis), because the absolute barrier thicknesses are nominal (see the text).

that the TMR is mainly caused by the carriers with large $k_\parallel$ ($>k_{\text{cutoff}}$). These carriers with larger $k_\parallel$ exponentially decay more rapidly during tunneling in the barrier because of larger κ_z, as shown in the middle of Fig. 3. Because of this in-plane dispersion of $\kappa_z(k_\parallel)$, when the barrier thickness d is large, the tunneling conductance is dominated by the carriers with smaller $k_\parallel$, which do not contribute much to the TMR. Therefore, the TMR decreases as d increases.

In order to quantitatively compare with our experiments, we calculated the dependence of TMR on d_{AlAs} in the spin-orbit nearest-neighbor sp^3s^* model [14,15]. We used tight-binding parameters in Ref. [16] to obtain the realistic band structures of GaAs and AlAs. The influence of Mn ions in $Ga_{1-x}Mn_xAs$ was taken into account by introducing an additional term ΔJ_x into the intralayer coupling matrices in the sp^3s^* Hamiltonian. Here J_x is a 10×10 matrix derived from the x component of the total angular momentum $\mathbf{J}$ in the planar-orbital basis. We used J_x because the magnetization was along the [100] axis. This additional term causes the changes in the on-site energies proportional to J_x. The scalar proportional coefficient Δ corresponds to the spin-splitting energy between the two holes $|\frac{3}{2}, \frac{1}{2}\rangle$ and $|\frac{3}{2}, -\frac{1}{2}\rangle$ at the Γ point.

Figure 4 shows the calculated (solid curve) and measured (solid circles) barrier thickness dependences of the TMR in the present $Ga_{1-x}Mn_xAs/AlAs/Ga_{1-x}Mn_xAs$ tunnel junctions. We assumed that E_F, V, and Δ were 0.2, 0.67, and 0.08 eV, respectively. E_F and V were measured from the top of the valence band in the calculated $Ga_{1-x}Mn_xAs$ band structure, as shown in the inset of Fig. 4. The valence band offset V is 0.67 eV for $Ga_{1-x}Mn_xAs/AlAs$ ($V = 0.55$ eV when $\Delta = 0$ for normal GaAs/AlAs interfaces, which is a reasonable value). Compared with the experimental results, the calculated TMR decreases rapidly in the thinner barrier region. Because completely accurate alignment of the moving shutter with the substrate in our MBE chamber is difficult, the absolute values of the evaluated barrier thickness may not be reliable (though the relative values are reliable), thus we horizontally shifted the calculated dependence towards the right by 0.7 nm (only 2.5 monolayers) to fit the experimental results, as shown by the dashed curve in Fig. 4. The fit is fairly good, but not perfect partly because the band structure of $Ga_{1-x}Mn_xAs$ is still unknown and the model is simple compared with the more complex band structure. However, the present spin-orbit nearest-neighbor sp^3s^* model explains well the most essential part of the experimental barrier thickness dependence of the TMR. Note that there are three essential points in this model: (i) The cutoff wave vector k_{cutoff} exists in the antiparallel configuration. (ii) The decaying factor κ_z in the barrier increases with increasing $k_\parallel$. (iii) $\mathbf{k}_\parallel$ is conserved in tunneling. Although these may not be valid in the conventional MTJs with polycrystalline metallic electrodes, we think that they are valid in the present epitaxial monocrystalline $Ga_{1-x}Mn_xAs/AlAs/Ga_{1-x}Mn_xAs$ tunnel junctions.

[1] T. Miyazaki and N. Tezuka, J. Magn. Magn. Mater. **139**, L231 (1995).
[2] J. S. Moodera *et al.,* Phys. Rev. Lett. **74**, 3273 (1995).
[3] M. Tanaka, J. Vac. Sci. Technol. B **16**, 2267 (1998); M. Tanaka, J. Vac. Sci. Technol. A **18**, 1247 (2000).
[4] H. Ohno, J. Magn. Magn. Mater. **200**, 110 (1999).
[5] Y. Ohno *et al.,* Nature (London) **402**, 790 (1999).
[6] T. Hayashi *et al.,* J. Appl. Phys. **87**, 4673 (2000).
[7] T. Hayashi *et al.,* J. Cryst. Growth **201/202**, 689 (1999).
[8] D. Chiba *et al.,* Appl. Phys. Lett. **77**, 1873 (2000).
[9] The valence band offset between $Ga_{1-x}Mn_xAs$ and AlAs is unknown but it is considered to be similar to that ($\sim$0.55 eV) of GaAs and AlAs, and the Fermi energy of holes in $Ga_{1-x}Mn_xAs$ is 0.1 $\sim$ 0.2 eV, thus the barrier height V_b is $\sim$0.45 eV. Therefore the effective mass m^* of holes which are responsible for tunneling is roughly estimated to be $\sim 0.7m_0$.
[10] Y. Higo, H. Shimizu, and M. Tanaka, J. Appl. Phys. **89**, 6745 (2001).
[11] C. H. Shang *et al.,* Phys. Rev. B **58**, R2917 (1998).
[12] M. Jullière, Phys. Lett. **54A**, 225 (1975).
[13] J. Mathon, Phys. Rev. B **56**, 11 810 (1997).
[14] P. Vogl *et al.,* J. Phys. Chem. Solids **44**, 365 (1983).
[15] D. J. Chadi, Phys. Rev. B **16**, 790 (1977).
[16] J. N. Schulman and Y.-C. Chang, Phys. Rev. B **31**, 2056 (1985).